

A combined immune-hypoxia model for predicting BRCA radiosensitivity

Table S1. Clinicopathologic characteristics of breast cancer in the TCGA dataset

Characteristic	TCGA		P value
	RT (n=540)	NRT (n=406)	
Age			
<60	305 (56.48%)	203 (50%)	0.048
≥60	235 (43.52%)	203 (50%)	
Histological type			
Lobular Carcinoma	110 (20.37%)	79 (19.46%)	0.218
Ductal Carcinoma	387 (71.67%)	281 (69.21%)	
Mixed	16 (2.96%)	11 (2.71%)	
Others	27 (5%)	34 (8.37%)	
NA	0	1 (0.25%)	
Pathological stage			
I/II	366 (67.78%)	329 (81.03%)	<0.001
III/IV	165 (30.56%)	67 (16.5%)	
NA	9 (1.67%)	10 (2.46%)	
ER			
ER-	111 (20.56%)	91 (22.41%)	0.504
ER+	406 (75.19%)	299 (73.65%)	
NA	23 (4.26%)	16 (3.94%)	
PR			
PR-	167 (30.93%)	125 (30.79%)	0.978
PR+	350 (64.81%)	263 (64.78%)	
NA	23 (4.26%)	18 (4.43%)	
HER2			
HER2-	280 (51.85%)	197 (48.52%)	0.141
HER2+/-	66 (12.22%)	68 (16.75%)	
HER2+	105 (19.44%)	76 (18.72%)	
NA	89 (16.48%)	65 (16.01%)	
Chemotherapy			
No	26 (4.81%)	62 (15.27%)	<0.001
Yes	486 (90%)	282 (69.46%)	
NA	28 (5.19%)	62 (15.27%)	
Status			
alive	491 (90.93%)	348 (85.71%)	0.012
death	49 (9.07%)	58 (14.29%)	
SurvTime (month)*	32.49 (18.61, 63.25)	23.98 (13.47, 52.13)	<0.001

*P50(P25, P75); RT, radiotherapy; NRT, non-radiotherapy; NA, data not available; ER, estrogen receptor; PR, progesterone receptor; HER2, human epidermal growth factor receptor 2.

Table S2. Clinicopathologic characteristics of breast cancer in the METABRIC dataset

Characteristic	METABRIC		P value
	RT (n=1137)	NRT (n=764)	
Age			
<60	555 (48.81%)	285 (37.3%)	<0.001
≥60	582 (51.19%)	479 (62.7%)	
Histological type			
Lobular Carcinoma	75 (6.6%)	67 (8.77%)	0.144
Ductal Carcinoma	885 (77.84%)	566 (74.08%)	
Mixed	115 (10.11%)	92 (12.04%)	
Others	53 (4.66%)	33 (4.32%)	

A combined immune-hypoxia model for predicting BRCA radiosensitivity

NA	9 (0.79%)	6 (0.79%)	
Grade			
I	82 (7.21%)	82 (10.73%)	<0.001
II	402 (35.36%)	338 (44.24%)	
III	627 (55.15%)	299 (39.14%)	
NA	26 (2.29%)	45 (5.89%)	
ER			
ER-	305 (26.82%)	138 (18.06%)	<0.001
ER+	832 (73.18%)	626 (81.94%)	
PR			
PR-	562 (49.43%)	331 (43.32%)	0.009
PR+	575 (50.57%)	433 (56.68%)	
HER2			
HER2-	990 (87.07%)	675 (88.35%)	0.407
HER2+	147 (12.93%)	89 (11.65%)	
Chemotherapy			
No	814 (71.59%)	691 (90.45%)	<0.001
Yes	323 (28.41%)	73 (9.55%)	
Status			
alive	530 (46.61%)	269 (35.21%)	<0.001
death	607 (53.39%)	495 (64.79%)	
SurvTime (month)*	116.63 (61.33, 182.93)	114.28 (60.89, 186.88)	0.818

*P50(P25, P75); RT, radiotherapy; NRT, non-radiotherapy; NA, data not available; ER, estrogen receptor; PR, progesterone receptor; HER2, human epidermal growth factor receptor 2.

Table S3. Clinicopathologic characteristics of breast cancer in the E-TABM-158 dataset

Characteristic	E-TABM-158		P value
	RT (n=59)	NRT (n=56)	
Age			
<60	42 (71.19%)	36 (64.29%)	0.429
≥60	17 (28.81%)	20 (35.71%)	
Pathological stage			
I/II	48 (81.36%)	45 (80.36%)	0.936
III/IV	10 (16.95%)	9 (16.07%)	
NA	1 (1.69%)	2 (3.57%)	
ER			
ER-	24 (40.68%)	19 (33.93%)	0.455
ER+	35 (59.32%)	37 (66.07%)	
PR			
PR-	26 (44.07%)	25 (44.64%)	0.984
PR+	32 (54.24%)	31 (55.36%)	
NA	1 (1.69%)	0	
Chemotherapy			
No	25 (42.37%)	29 (51.79%)	0.312
Yes	34 (57.63%)	27 (48.21%)	
DSS			
alive	44 (74.58%)	44 (78.57%)	0.613
death	15 (25.42%)	12 (21.43%)	
SurvTime (month)*	81.12 (45.18, 117.90)	72.60 (36.06, 108.84)	0.339

*P50(P25, P75); RT, radiotherapy; NRT, non-radiotherapy; NA, data not available; ER, estrogen receptor; PR, progesterone receptor; DSS, disease-specific survival.

A combined immune-hypoxia model for predicting BRCA radiosensitivity

Table S4. Clinicopathologic characteristics of breast cancer in the GSE103746 dataset

Characteristic	GSE103746		P value
	RT (n=118)	NRT (n=54)	
ER			
ER-	38 (32.20%)	12 (22.22%)	0.181
ER+	80 (67.80%)	42 (77.78%)	
NA			
Reference			
no	68 (57.63%)	36 (66.67%)	0.261
yes	50 (42.37%)	18 (33.33%)	
Follow-up time (month)*	104.89 (46.46, 166.07)	132.44 (61.60, 180.70)	0.373

*P50(P25, P75); RT, radiotherapy; NRT, non-radiotherapy.

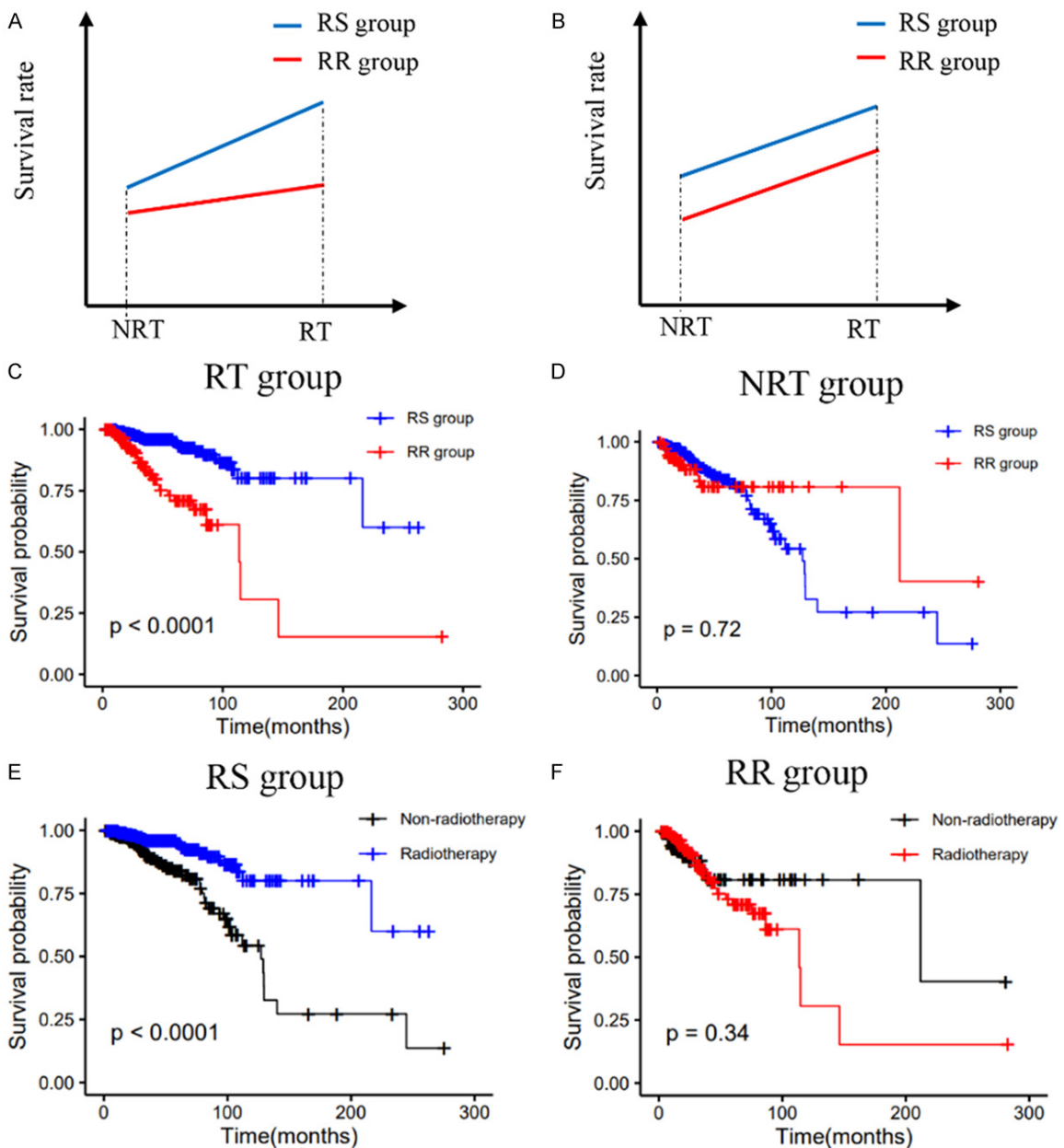


Figure S1. Definition of radiosensitivity and radiosensitivity gene signature.

A combined immune-hypoxia model for predicting BRCA radiosensitivity

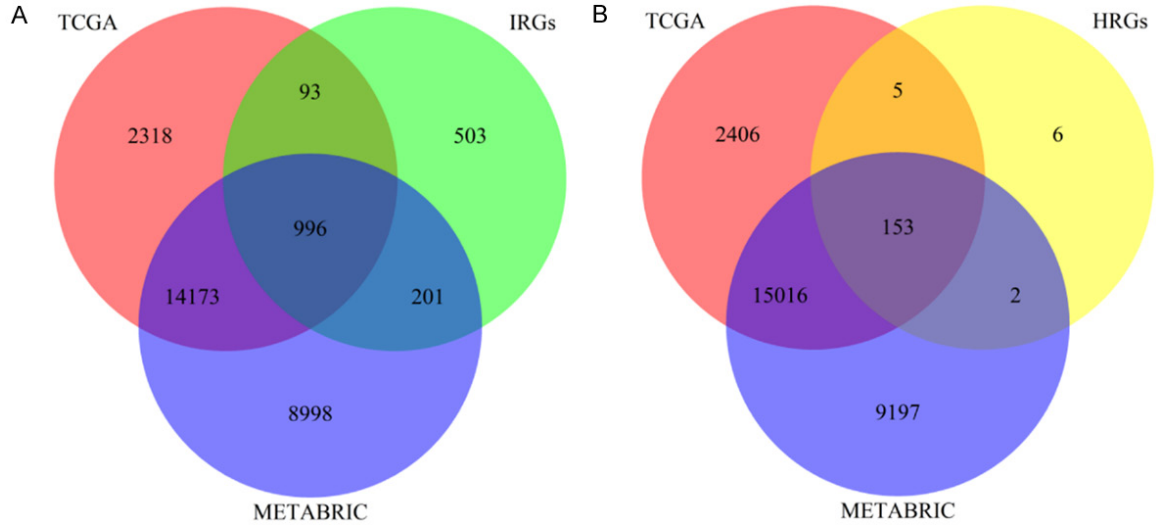


Figure S2. Venn diagram. The common immune-related genes (A) and hypoxia-related genes; (B) in the TCGA dataset, METABRIC datasets.

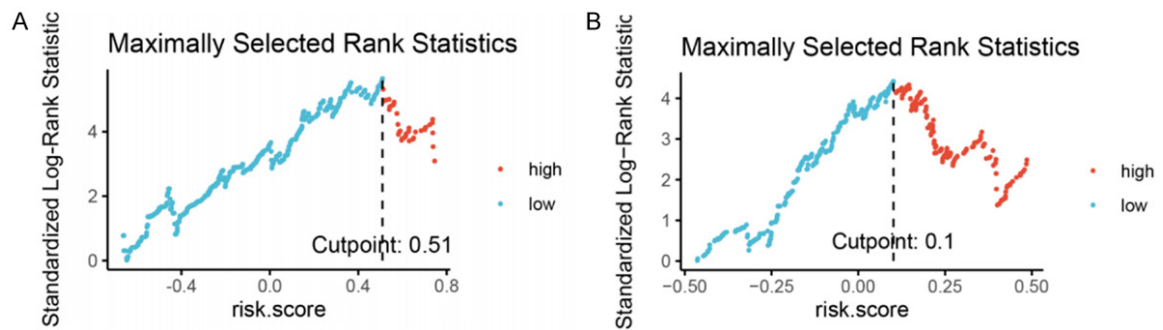


Figure S3. The optional cutoff values were determined by maximally selected rank statistics. A. Immune signature; B. Hypoxia signature.

Table S5. Univariate Cox regression analysis of radiotherapy and non-radiotherapy patients in the TCGA dataset

Gene names	Radiotherapy for all patients		Non-radiotherapy for all patients	
	HR (95% CI)	P value	HR (95% CI)	P value
IRGs				
ACVRL1	1.371 (1.139-1.649)	0.001	0.913 (0.679-1.226)	0.543
ADM	1.277 (1.115-1.462)	<0.001	1.193 (0.835-1.703)	0.332
ADRM1	1.225 (1.060-1.417)	0.006	1.146 (0.84-1.562)	0.39
AIMP1	1.099 (1.034-1.169)	0.003	1.144 (0.415-3.155)	0.795
AKT1	1.267 (1.020-1.573)	0.033	0.995 (0.754-1.314)	0.973
ANGPTL6	1.231 (1.035-1.463)	0.019	1.081 (0.779-1.501)	0.64
ARRB1	1.336 (1.041-1.715)	0.023	0.837 (0.479-1.464)	0.533
BMP1	1.250 (1.121-1.395)	<0.001	1.012 (0.658-1.555)	0.957
BMPR1A	0.650 (0.457-0.924)	0.016	0.949 (0.735-1.227)	0.69
BRAF	0.449 (0.277-0.729)	0.001	0.978 (0.734-1.304)	0.88
CBL	0.723 (0.523-0.999)	0.049	1.163 (0.854-1.585)	0.337
CCL26	1.359 (1.051-1.759)	0.019	0.893 (0.473-1.687)	0.727
CD14	1.216 (1.089-1.357)	<0.001	0.996 (0.738-1.343)	0.978
CD320	1.199 (1.003-1.432)	0.046	0.996 (0.733-1.354)	0.98

A combined immune-hypoxia model for predicting BRCA radiosensitivity

CD81	1.368 (1.136-1.646)	0.001	0.984 (0.774-1.251)	0.895
CMKLR1	1.288 (1.045-1.587)	0.018	0.77 (0.506-1.171)	0.221
CMTM6	0.625 (0.426-0.916)	0.016	0.808 (0.621-1.053)	0.115
CXCL1	1.353 (1.008-1.816)	0.044	0.391 (0.126-1.215)	0.105
CXCL16	0.559 (0.348-0.897)	0.016	0.893 (0.66-1.21)	0.466
DLL4	1.319 (1.105-1.576)	0.002	1.081 (0.838-1.393)	0.55
EDN2	1.335 (1.077-1.655)	0.008	0.922 (0.705-1.207)	0.556
ENG	1.383 (1.136-1.683)	0.001	0.825 (0.595-1.145)	0.25
ESRRA	1.271 (1.001-1.612)	0.049	1.262 (0.968-1.644)	0.085
F2RL1	1.293 (1.050-1.593)	0.016	1.103 (0.869-1.399)	0.42
FAM3D	1.200 (1.088-1.323)	<0.001	0.806 (0.432-1.503)	0.497
FCGRT	1.263 (1.015-1.571)	0.036	0.941 (0.703-1.26)	0.685
FIGNL2	1.359 (1.117-1.654)	0.002	0.982 (0.751-1.284)	0.895
FLT4	1.235 (1.024-1.490)	0.027	0.834 (0.589-1.182)	0.308
GDF11	1.283 (1.040-1.582)	0.02	0.924 (0.666-1.282)	0.637
GDF3	1.213 (1.007-1.462)	0.042	1.185 (0.871-1.612)	0.279
GFAP	1.257 (1.080-1.462)	0.003	0.689 (0.355-1.338)	0.271
GRN	1.216 (1.014-1.458)	0.035	1.084 (0.792-1.482)	0.614
HRAS	1.249 (1.000-1.559)	0.05	0.932 (0.652-1.333)	0.701
IL1A	1.197 (1.099-1.303)	<0.001	0.378 (0.052-2.767)	0.338
IL31RA	1.240 (1.092-1.406)	0.001	1.135 (0.816-1.577)	0.452
KLRC2	0.208 (0.047-0.920)	0.039	1.09 (0.876-1.355)	0.44
KLRC3	0.118 (0.021-0.646)	0.014	1.018 (0.892-1.161)	0.793
LGR4	1.226 (1.001-1.501)	0.049	0.876 (0.641-1.197)	0.405
LMBR1L	1.371 (1.053-1.785)	0.019	0.999 (0.758-1.317)	0.996
MAP2K2	1.267 (1.012-1.586)	0.039	0.942 (0.676-1.313)	0.726
MMP9	1.160 (1.076-1.250)	<0.001	0.27 (0.012-6.208)	0.413
MUC4	14.333 (2.951-69.624)	0.001	0.941 (0.534-1.659)	0.833
NCK1	0.550 (0.352-0.859)	0.009	0.998 (0.798-1.248)	0.984
NFAT5	0.682 (0.475-0.980)	0.039	0.973 (0.729-1.299)	0.852
NR1D1	1.168 (1.002-1.360)	0.047	1.046 (0.808-1.353)	0.734
NR1H2	1.433 (1.121-1.832)	0.004	0.936 (0.718-1.22)	0.624
NR2F1	1.155 (1.021-1.308)	0.023	0.783 (0.441-1.39)	0.404
OGFR	1.330 (1.045-1.692)	0.021	0.827 (0.606-1.127)	0.228
PAK6	1.475 (1.195-1.821)	<0.001	1.166 (0.931-1.462)	0.181
PDGFRB	1.402 (1.127-1.743)	0.002	1.094 (0.807-1.482)	0.564
PGF	1.273 (1.147-1.412)	<0.001	1.169 (0.865-1.58)	0.31
PIK3CA	1.137 (1.063-1.215)	<0.001	1.38 (0.616-3.094)	0.434
PLAU	1.252 (1.064-1.473)	0.007	1.266 (0.939-1.708)	0.122
PLTP	1.199 (1.072-1.340)	0.001	1.234 (0.94-1.619)	0.13
PLXND1	1.726 (1.377-2.164)	<0.001	1.138 (0.907-1.429)	0.263
PPARA	0.541 (0.349-0.840)	0.006	1.047 (0.848-1.292)	0.668
PSMC6	1.238 (1.033-1.485)	0.021	0.782 (0.528-1.159)	0.221
PTGDS	1.152 (1.071-1.239)	<0.001	0.228 (0.04-1.312)	0.098
PTGER1	1.283 (1.089-1.510)	0.003	0.907 (0.562-1.464)	0.689
QRFP	1.330 (1.106-1.599)	0.002	1.019 (0.754-1.378)	0.904
RABEP2	1.284 (1.007-1.638)	0.044	0.954 (0.675-1.349)	0.791
RAET1E	1.427 (1.104-1.843)	0.007	1.119 (0.74-1.693)	0.595
RFX5	0.667 (0.459-0.971)	0.035	0.998 (0.779-1.28)	0.989
RNASE7	1.177 (1.045-1.325)	0.007	0.557 (0.24-1.292)	0.173
RXFP1	1.222 (1.005-1.486)	0.044	0.94 (0.621-1.423)	0.771

A combined immune-hypoxia model for predicting BRCA radiosensitivity

S100A3	1.297 (1.170-1.437)	<0.001	0.881 (0.596-1.303)	0.526
SEMA7A	1.514 (1.298-1.767)	<0.001	0.886 (0.598-1.314)	0.547
SOD1	1.284 (1.044-1.579)	0.018	1.08 (0.875-1.333)	0.473
STAT3	0.681 (0.475-0.976)	0.036	0.94 (0.722-1.226)	0.649
TGFB1	1.195 (1.018-1.402)	0.03	0.736 (0.502-1.079)	0.117
TGFB2	0.459 (0.256-0.823)	0.009	1.053 (0.791-1.403)	0.722
THPO	1.340 (1.037-1.731)	0.025	0.968 (0.804-1.164)	0.729
TIE1	1.224 (1.020-1.470)	0.03	0.896 (0.646-1.241)	0.508
TINAGL1	1.382 (1.080-1.768)	0.01	1.084 (0.86-1.366)	0.497
TMSB10	1.325 (1.075-1.633)	0.008	0.96 (0.707-1.304)	0.794
TNFRSF4	1.392 (1.154-1.678)	0.001	0.866 (0.62-1.209)	0.397
TNFRSF6B	1.268 (1.107-1.452)	0.001	0.734 (0.475-1.134)	0.164
TOR2A	1.347 (1.045-1.735)	0.021	0.932 (0.706-1.23)	0.618
TRPC4AP	1.185 (1.026-1.368)	0.021	0.978 (0.626-1.526)	0.921
UNC93B1	1.236 (1.052-1.452)	0.01	1.081 (0.833-1.404)	0.556
VIP	1.215 (1.054-1.400)	0.007	0.73 (0.472-1.129)	0.157
HRGs				
BGN	1.205 (1.012-1.434)	0.036	1.005 (0.696-1.451)	0.978
CDKN1A	1.283 (1.012-1.625)	0.039	0.822 (0.567-1.191)	0.301
CP	1.253 (1.074-1.462)	0.004	1.096 (0.832-1.443)	0.516
GBE1	0.648 (0.428-0.981)	0.04	1.06 (0.863-1.301)	0.579
GPC1	1.195 (1.061-1.345)	0.003	1.008 (0.581-1.749)	0.978
KDM3A	0.624 (0.404-0.964)	0.033	1.188 (0.982-1.436)	0.076
MT2A	1.247 (1.035-1.503)	0.02	0.775 (0.504-1.192)	0.246
NAGK	1.326 (1.030-1.706)	0.028	1.2 (0.98-1.47)	0.078
PRDX5	1.288 (1.042-1.591)	0.019	1.046 (0.801-1.367)	0.741
S100A4	1.162 (1.043-1.294)	0.007	1.045 (0.691-1.582)	0.833
SERPINE1	1.311 (1.169-1.471)	<0.001	0.817 (0.57-1.172)	0.273
SLC25A1	1.332 (1.014-1.751)	0.039	1.05 (0.824-1.337)	0.694
SRPX	1.355 (1.163-1.578)	<0.001	0.92 (0.611-1.387)	0.692
TGFBI	1.296 (1.143-1.470)	<0.001	1.112 (0.768-1.61)	0.575

Table S6. Coefficients of spike-and-slab Lasso Cox and Lasso Cox models

Gene names	Coefficients
IRGs	
PAK6	0.364613574
PLXND1	0.435054147
SEMA7A	0.251088237
HRGs	
BGN	0.020302494
CP	0.207320903
GBE1	-0.373751049
GPC1	0.031078184
KDM3A	-0.032321533
NAGK	0.005800813
S100A4	0.083597029
SERPINE1	0.199830708
SLC25A1	0.117815068
SRPX	0.108774567
TGFBI	0.000371747

A combined immune-hypoxia model for predicting BRCA radiosensitivity

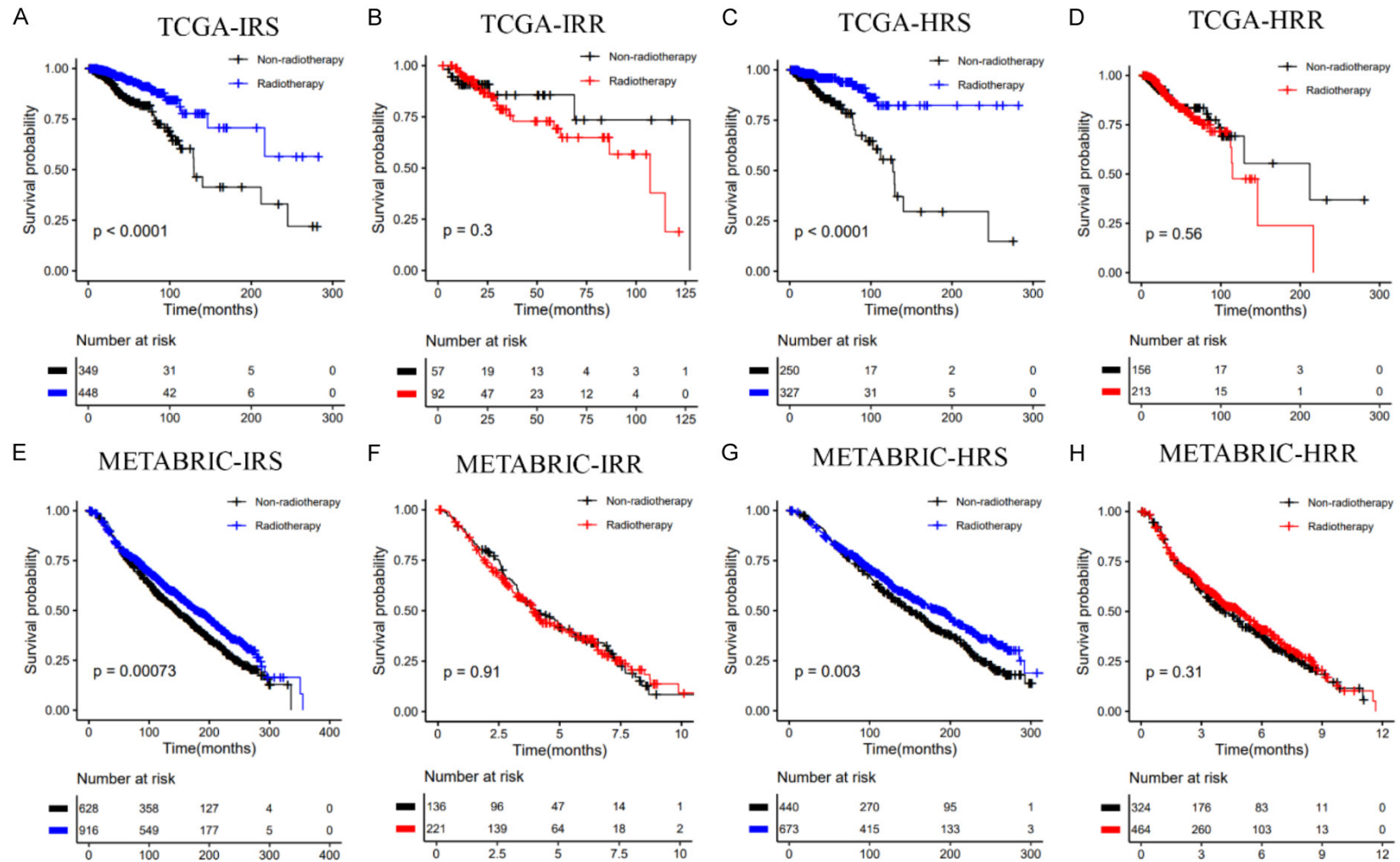


Figure S4. Kaplan-Meier curves of OS for patients who had received radiation vs. those who did not: A. TCGA-IRS group; B. TCGA-IRR group; C. TCGA-HRS group; D. TCGA-HRR group; E. METABRIC-IRS group; F. METABRIC-IRR group; G. METABRIC-HRS group; H. METABRIC-HRR group.

A combined immune-hypoxia model for predicting BRCA radiosensitivity

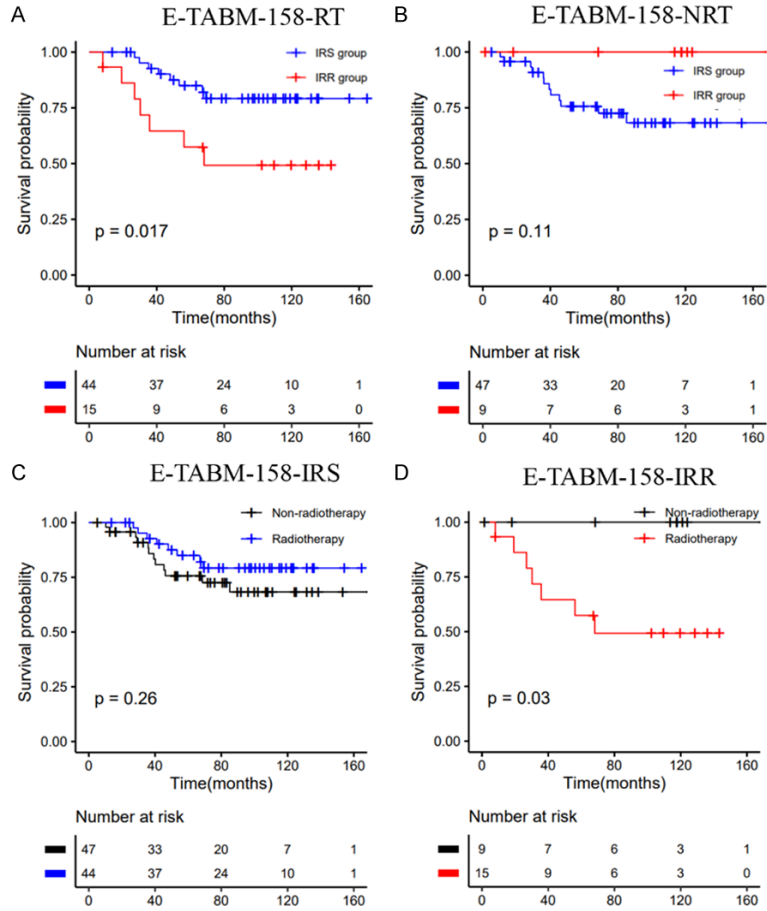


Figure S5. Disease-specific survival stratified by the immune signatures in the E-TABM-158 dataset.

A combined immune-hypoxia model for predicting BRCA radiosensitivity

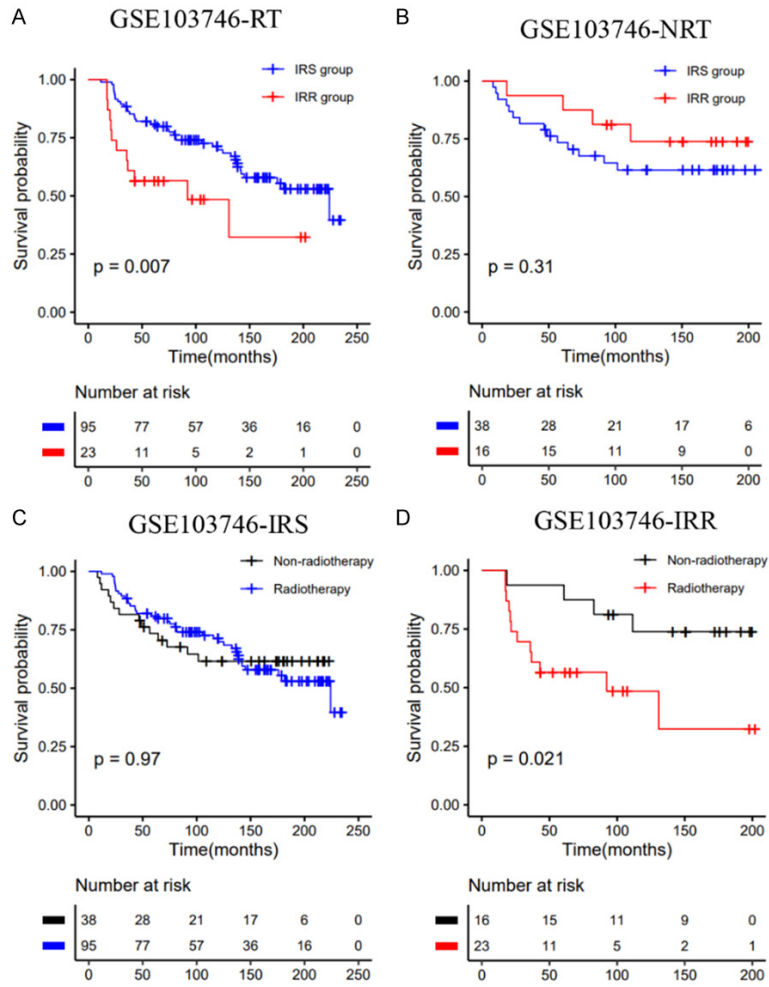


Figure S6. Recurrence-free survival stratified by the immune signatures in the GSE103746 dataset.

A combined immune-hypoxia model for predicting BRCA radiosensitivity

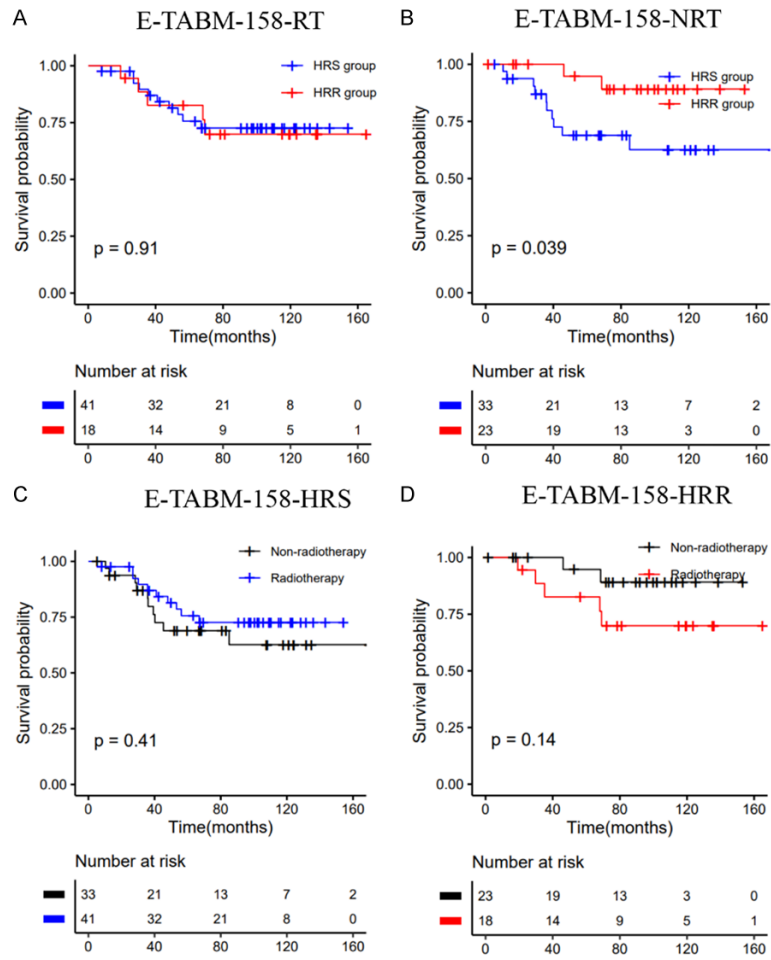


Figure S7. Recurrence-free survival stratified by the hypoxia signatures in the E-TABM-158 dataset.

A combined immune-hypoxia model for predicting BRCA radiosensitivity

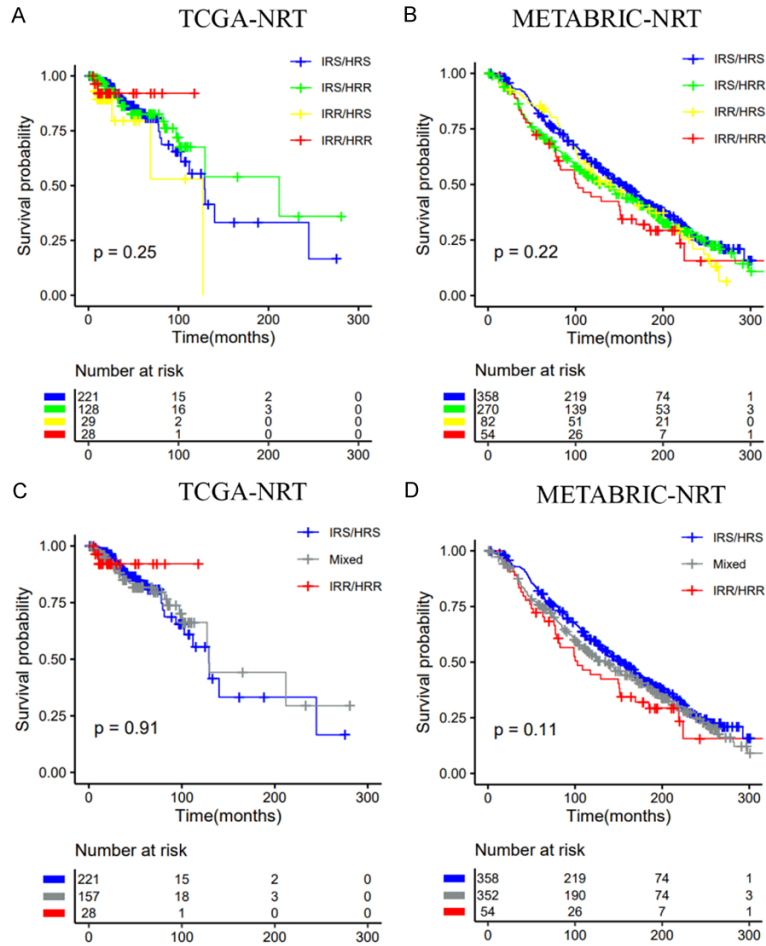


Figure S8. Classification of nonradiotherapy patients into subgroups according to the immune signature (IRS vs. IRR) and the hypoxia signature (HRS vs. HRR). A, C. TCGA dataset; B, D. METABRIC dataset.

A combined immune-hypoxia model for predicting BRCA radiosensitivity

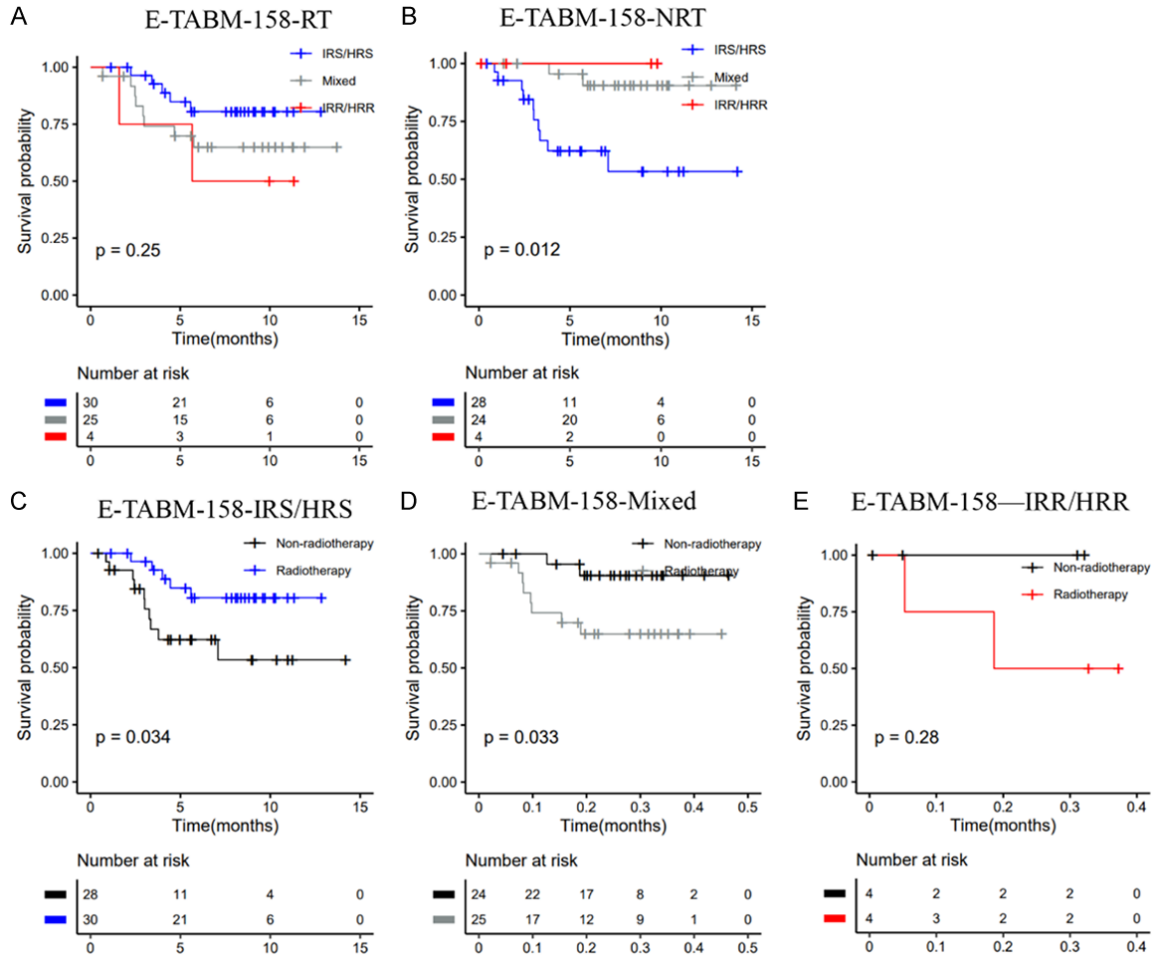


Figure S9. Classification of patients into subgroups according to the immune signature (IRS vs. IRR) and the hypoxia signature (HRS vs. HRR) in the E-TABM-158 dataset.

A combined immune-hypoxia model for predicting BRCA radiosensitivity

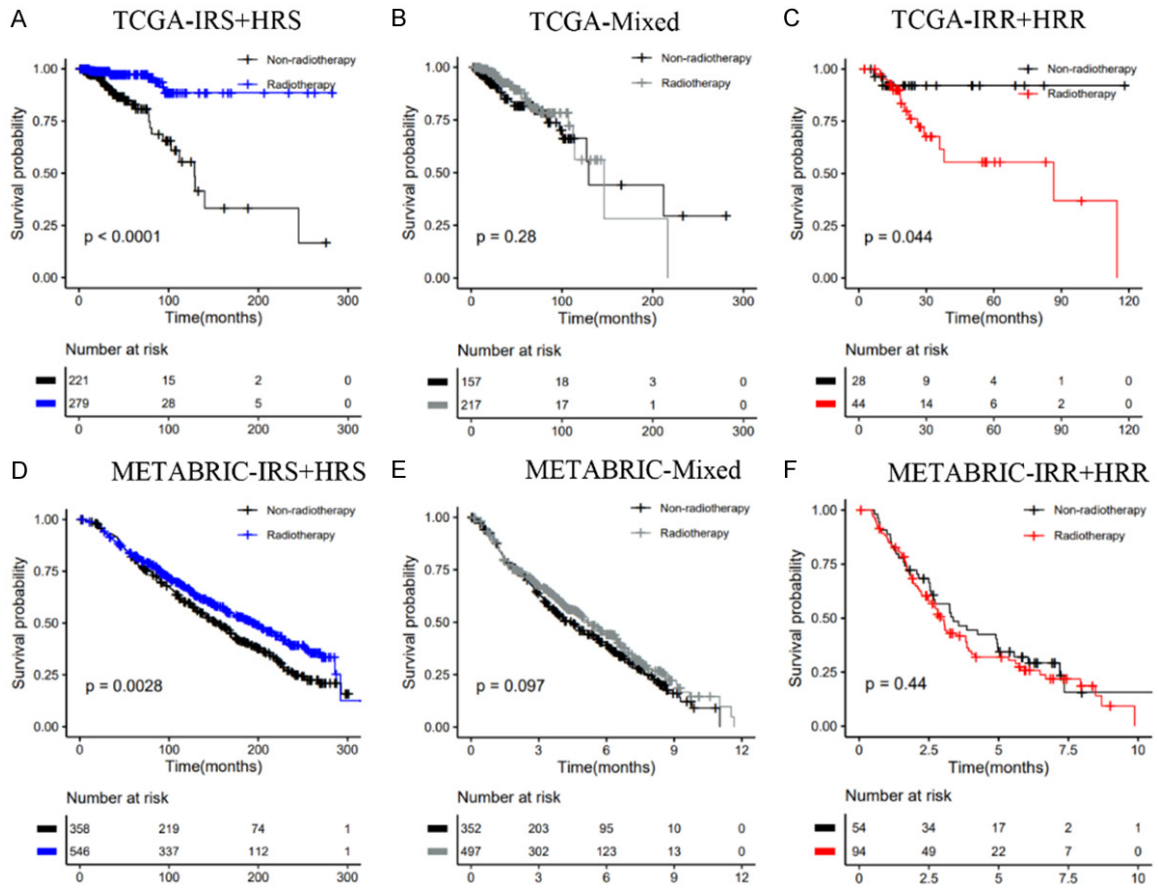


Figure S10. Overall survival stratified by the combination of immune and hypoxia gene signatures. A-C. TCGA dataset; D-F. METABRIC dataset.

A combined immune-hypoxia model for predicting BRCA radiosensitivity

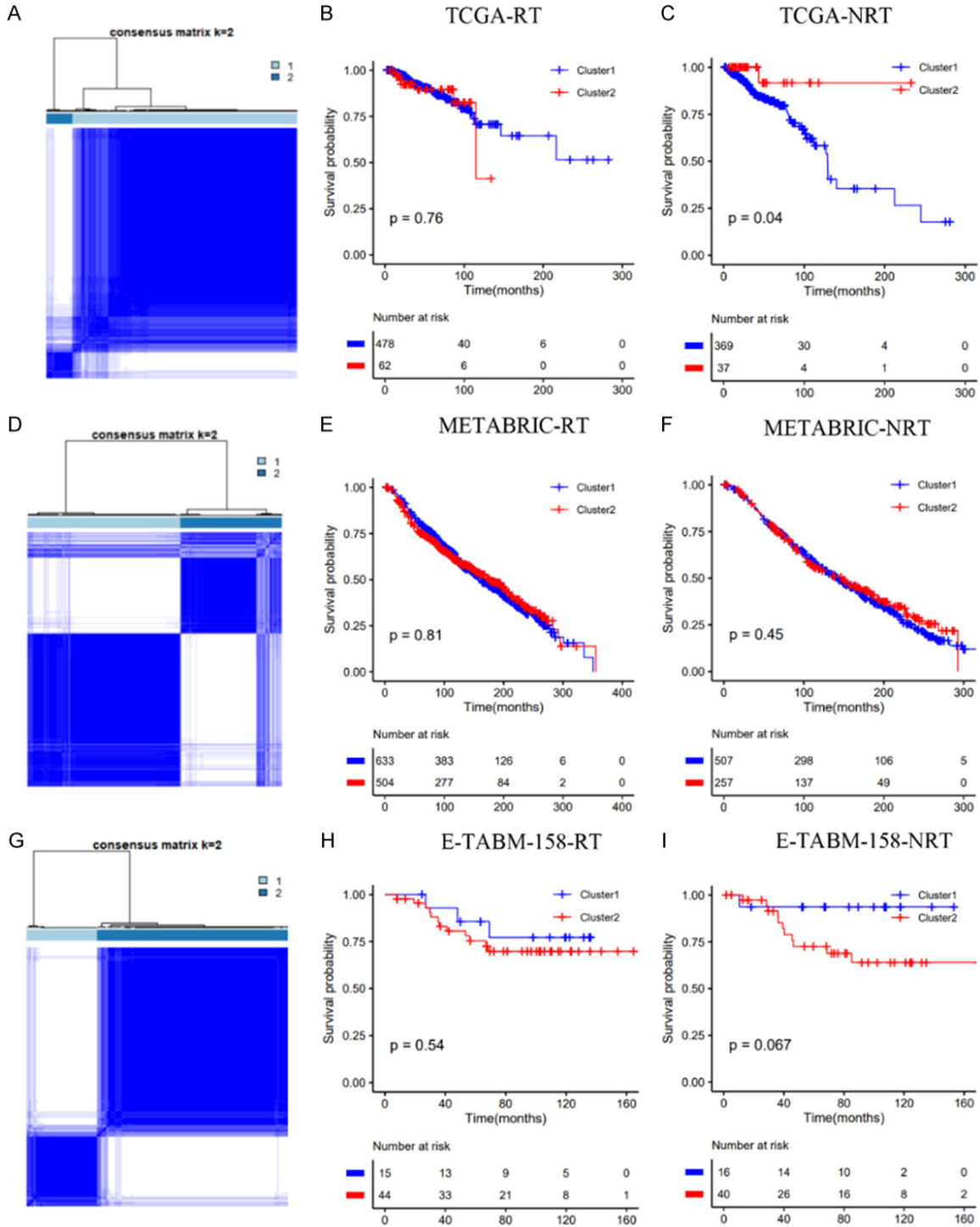


Figure S11. Validation of 31-gene in the TCGA, METABRIC, E-TABM-158 datasets. A, D, G. Consensus clustering algorithm generated two clusters based on the expression profile of the 31-gene signature; B, C. Kaplan-Meier plot of OS for the two clusters in the TCGA dataset; E, F. Kaplan-Meier plot of OS for the two clusters in the METABRIC dataset; H, I. Kaplan-Meier plot of DSS for the two clusters in the E-TABM-158 dataset.

A combined immune-hypoxia model for predicting BRCA radiosensitivity

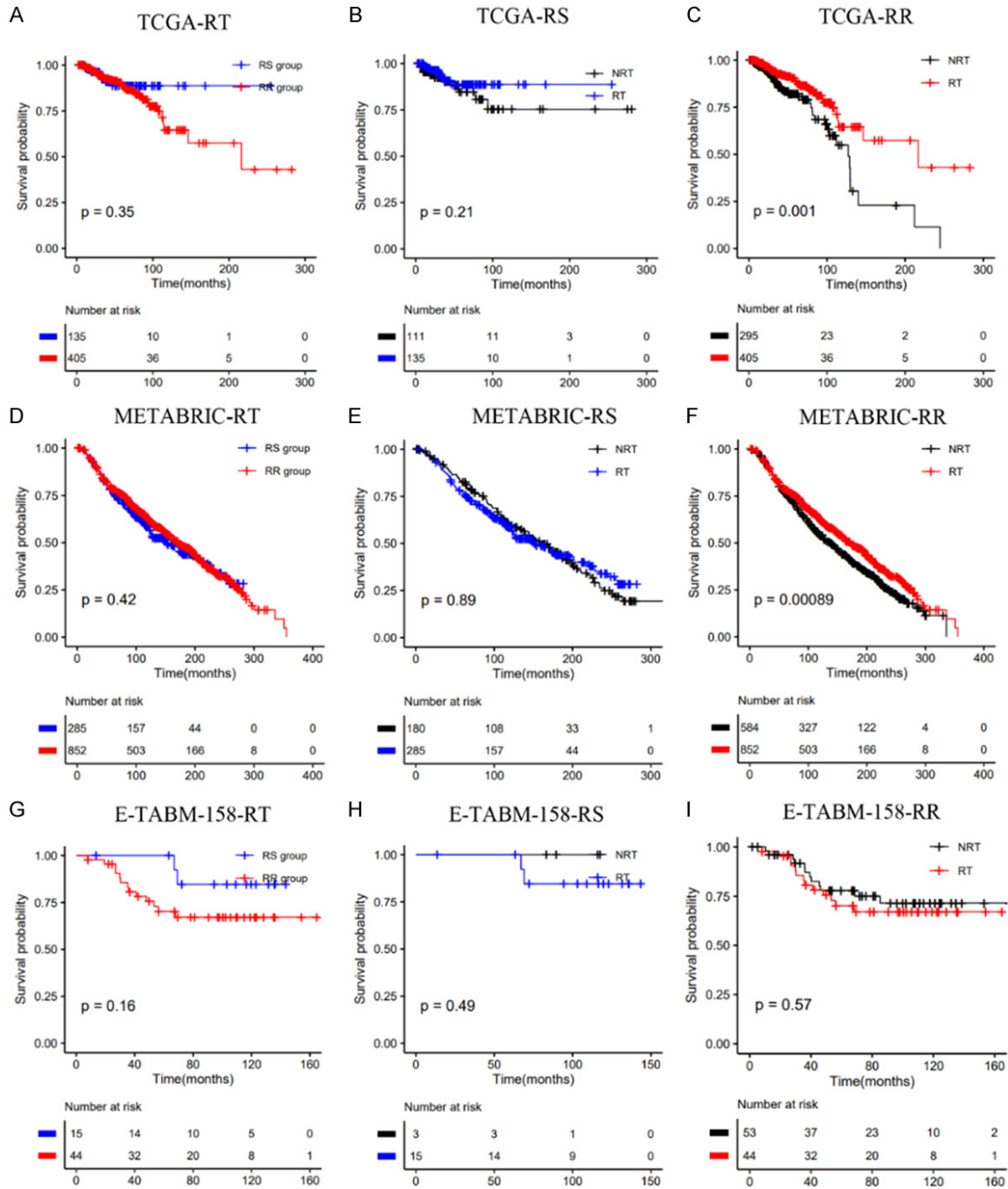
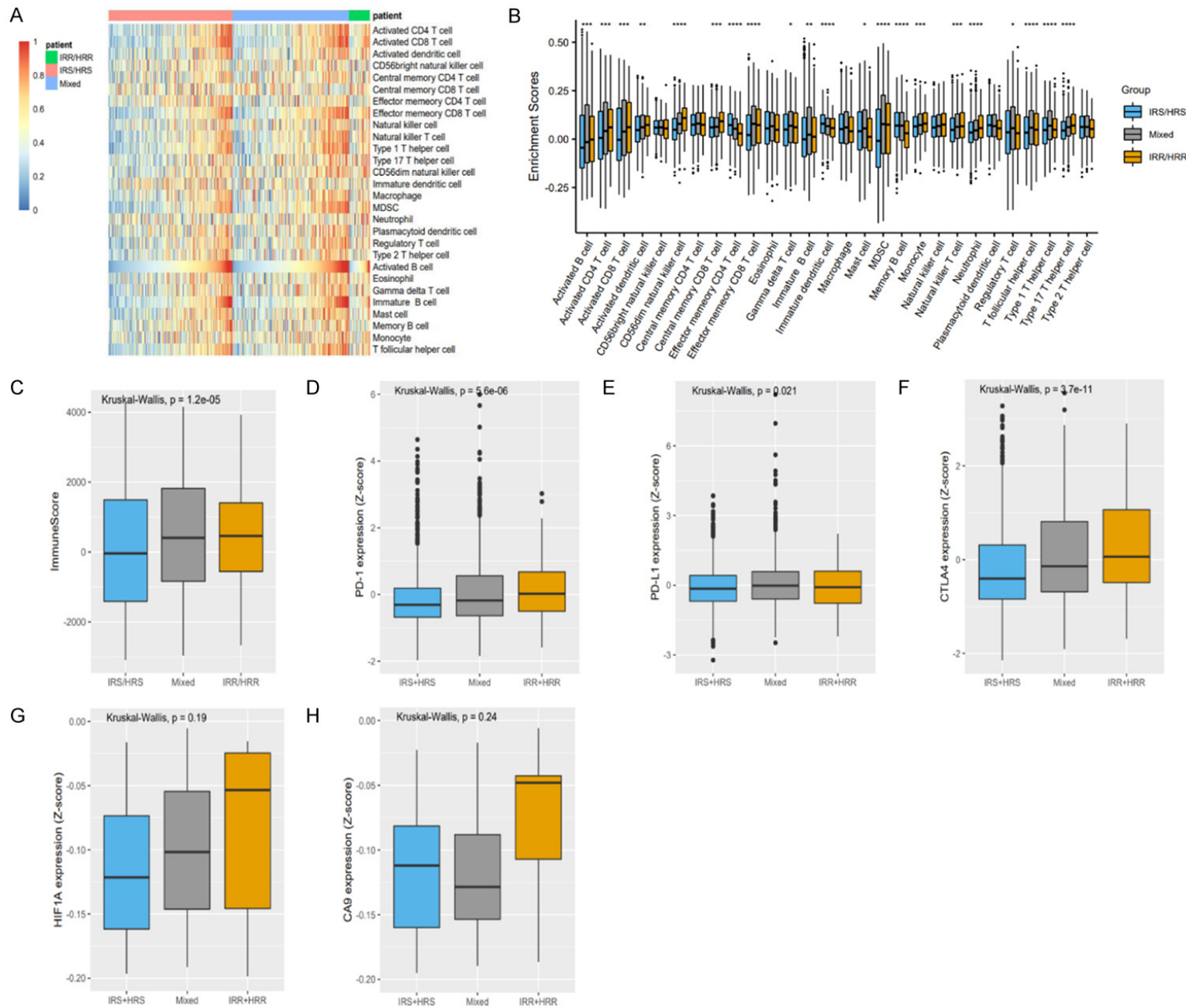


Figure S12. Validation of RSI in the TCGA, METABRIC, E-TABM-158 datasets.

A combined immune-hypoxia model for predicting BRCA radiosensitivity



A combined immune-hypoxia model for predicting BRCA radiosensitivity

Figure S13. Immune microenvironment of these three groups (IRS/HRS, Mixed, IRR/HRR) in the METABRIC dataset. A, B. ssGSEA analysis showed the immune cell proportions of three groups; C-F. Comparison of immune score, PD-1, PDL-1, CTLA-4 levels of three groups in all patients; G, H. Comparison of HIF-a, CA9 expression levels of three groups in radiotherapy patients.

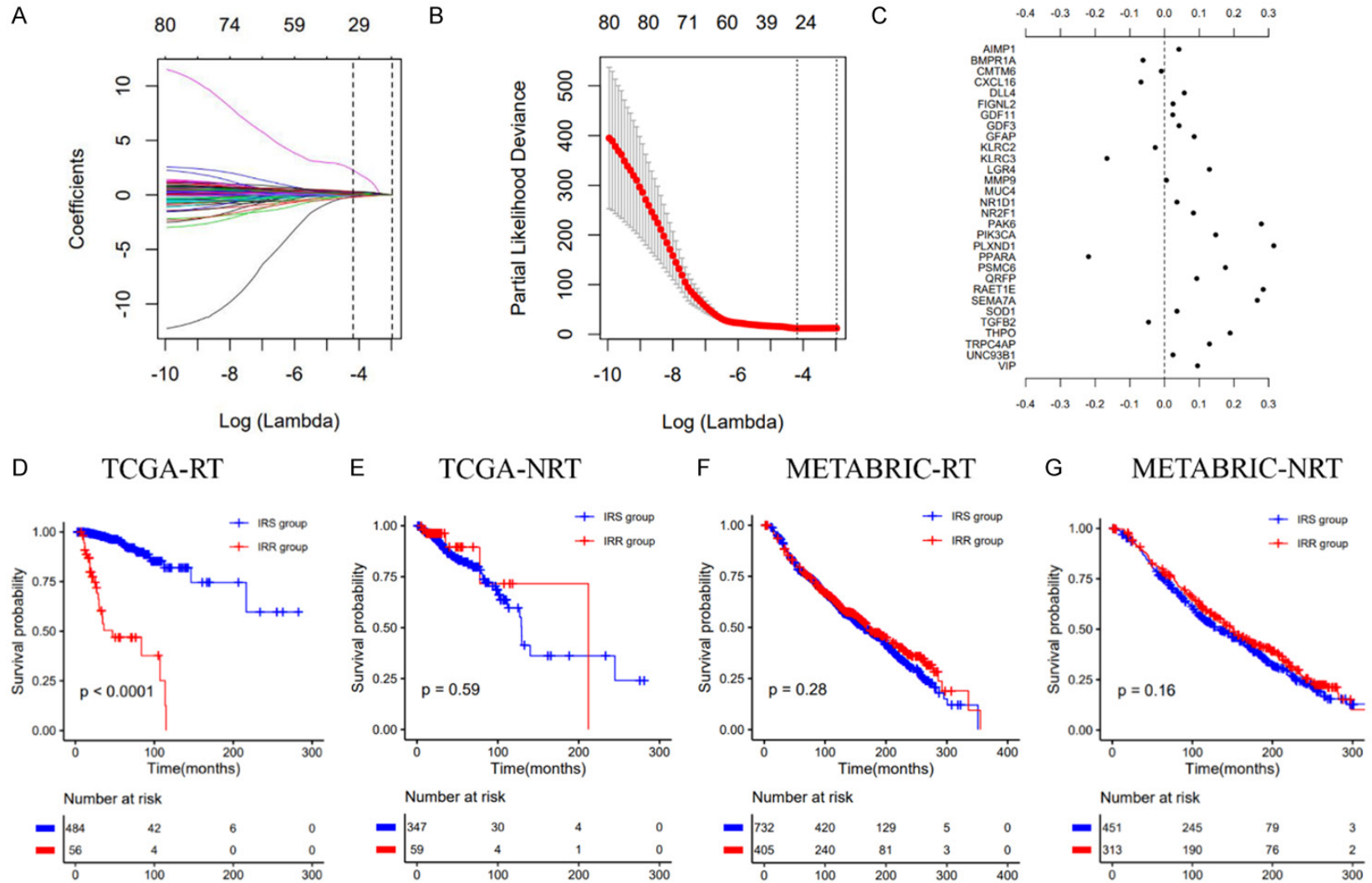


Figure S14. A-C. Candidate immune genes selection by Lasso Cox analysis; D-G. Kaplan-Meier survival curves of the IRS group and IRR group in radiotherapy patients and non-radiotherapy patients, respectively.

A combined immune-hypoxia model for predicting BRCA radiosensitivity

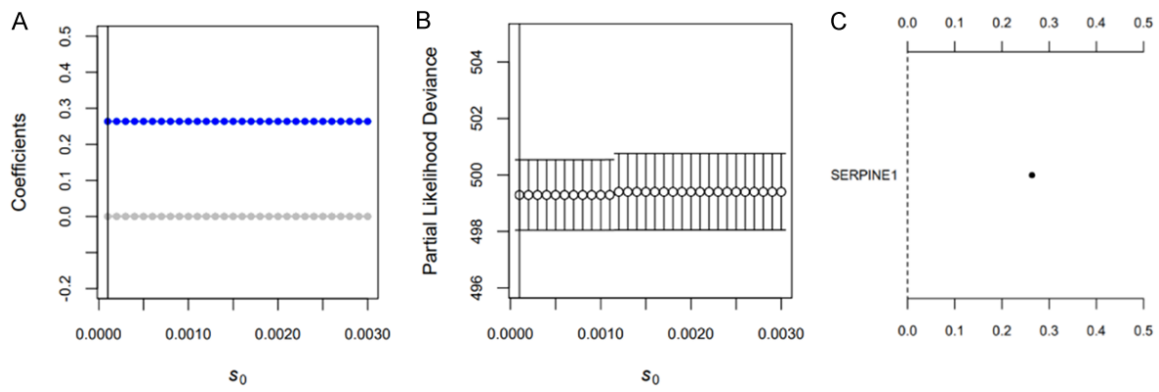


Figure S15. A-C. Candidate hypoxia genes selection by spike-and-slab Lasso Cox analysis.